

# A Generic Method for Fine-grained Category Discovery in Natural Language Texts

Chang Tian<sup>†</sup>, Matthew B. Blaschko<sup>†</sup>, Wenpeng Yin, Mingzhe Xing,  
Yinliang Yue, Marie-Francine Moens<sup>†</sup>

<sup>†</sup> KU Leuven

chang.tian@kuleuven.be

## Abstract

Fine-grained category discovery using only coarse-grained supervision is a cost-effective yet challenging task. Previous training methods focus on aligning query samples with positive samples and distancing them from negatives. They often neglect intra-category and inter-category semantic similarities of fine-grained categories when navigating sample distributions in the embedding space. Furthermore, some evaluation techniques that rely on pre-collected test samples are inadequate for real-time applications. To address these shortcomings, we introduce a method that successfully detects fine-grained clusters of semantically similar texts guided by a novel objective function. The method uses semantic similarities in a logarithmic space to guide sample distributions in the Euclidean space and to form distinct clusters that represent fine-grained categories. We also propose a centroid inference mechanism to support real-time applications. The efficacy of the method is both theoretically justified and empirically confirmed on three benchmark tasks. The proposed objective function is integrated in multiple contrastive learning based neural models. Its results surpass existing state-of-the-art approaches in terms of Accuracy, Adjusted Rand Index and Normalized Mutual Information of the detected fine-grained categories. Code and data will be available at <https://github.com/XX> upon publication.

## 1 Introduction

Fine-grained analysis has drawn much attention in many artificial intelligence fields, e.g., Computer Vision (Chen et al., 2018; Wang et al., 2024a; Park and Ryu, 2024) and Natural Language Processing (Ma et al., 2023; Tian et al., 2024; An et al., 2024), because it can provide more detailed features than coarse-grained data. For instance, as illustrated in Figure 1, solely based on coarse-grained analysis, the chatbot might incorrectly recommend a roadster, which is unsuitable for field

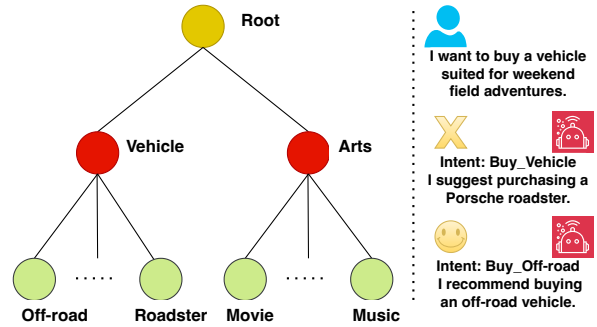


Figure 1: A fine-grained intent detection example. **Left:** This panel illustrates the label hierarchy, transitioning from coarse-grained to fine-grained granularity. **Right:** This example demonstrates intent detection in a conversation about car choices, showing how coarse-grained analysis alone can lead to incorrect recommendations by a life assistant due to a lack of fine-grained analysis.

adventures. Detecting the fine-grained intent would allow the chatbot to recommend an off-road vehicle that aligns with the user’s requirements. However, annotating fine-grained categories can be labor-intensive, as it demands precise expert knowledge specific to each domain and involved dataset. Addressing this challenge, An et al. (2022) recently introduced Fine-grained Category Discovery under Coarse-grained Supervision (FCDC) for language classification tasks (details in Section 3). FCDC aims to reduce annotation costs by leveraging the relative ease of obtaining coarse-grained annotations, without requiring fine-grained supervisory information. This approach has sparked significant research interest in the automatic discovery of fine-grained language categories. (Ma et al., 2023; An et al., 2023a; Vaze et al., 2024; Lian et al., 2024).

Existing methods for addressing FCDC are typically grouped into three groups (An et al., 2024): language models, self-training methods, and contrastive learning methods. Language models (Devlin et al., 2019a; Touvron et al., 2023), including their fine-tuned versions with coarse labels, gener-

ally perform poorly on this task due to a lack of fine-grained supervision. Self-training methods (Caron et al., 2018; Zhang et al., 2021) and their variants often employ clustering assignments as fine-grained pseudo labels, filtering out some noisy pseudo labels, and training with these labels. Dominant contrastive learning methods (Chen et al., 2020; Mekala et al., 2021; An et al., 2022, 2023a) typically identify positive and negative samples for a given query by measuring their semantic distances. The contrastive loss ensures that the query sample moves closer to positive samples and further away from negative samples. So these methods form clusters of samples in the embedding space, with each cluster representing a discovered fine-grained category, without requiring fine-grained category supervision.

However, past methods did not utilize **comprehensive semantic similarities (CSS)** in the logarithmic space to guide sample distributions in Euclidean space. We define CSS as the fine-grained semantic similarities measured by bidirectional KL divergence in the logarithmic space between the query sample and each available positive or negative sample, as illustrated in Figure 2. Although An et al. (2024) recently explored similarities measured by rank order between the query sample and positive samples, they ignore similarities with negative samples.

We propose a method (**STAR**) for detecting fine-grained clusters of semantically similar texts through a novel objective function, with the core component considering CSS. This component guides sample distributions in the Euclidean space based on the magnitude of CSS in the logarithmic space. Large semantic differences (low similarity) in the logarithmic space between the query sample and an available sample push the query sample further away in Euclidean space, while small semantic differences bring the query sample closer to the available sample. Thus, samples form distinguishable fine-grained clusters in Euclidean space, with each cluster representing a discovered category.

Additionally, clustering inference used by previous works (An et al., 2022, 2023a, 2024) can not support real-time scenarios, so we propose a variant inference mechanism utilizing approximated fine-grained cluster centroids, delivering competitive results for the tasks considered.

Our main contributions in this work can be summarized as follows:

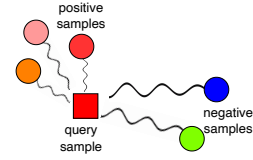


Figure 2: Visualization of comprehensive semantic similarities (CSS). The wavy line indicates the bidirectional KL divergence between two samples.

- **Method:** STAR enhances existing contrastive learning methods by leveraging comprehensive semantic similarities in a logarithmic space to guide sample distributions in the Euclidean space, thereby making fine-grained categories more distinguishable.
- **Theory:** We interpret STAR from the perspectives of clustering and generalized Expectation Maximization (EM). Also, we conduct loss and gradient analyses to explain the effectiveness of using CSS for category discovery.
- **Experiments:** Experiments on three text classification tasks (intent detection (Larson et al., 2019), scientific abstract classification (Kowsari et al., 2017), and chatbot query (Liu et al., 2021)) demonstrate new state-of-the-art (SOTA) performance compared to 22 baselines, validating the theoretical method.

## 2 Related Work

### 2.1 Fine-grained Category Discovery

Fine-grained data analysis is crucial in Natural Language Processing (Guo et al., 2021; Ma et al., 2023; Tian et al., 2024) and Computer Vision (Pan et al., 2023; Wang et al., 2024b). However, effectively discovering fine-grained categories from coarse-grained ones remains challenging (Mekala et al., 2021). Traditional category discovery methods often assume that known and discovered categories are at the same granularity level (An et al., 2023b; Vaze et al., 2024).

To discover fine-grained categories under the supervision of coarse-grained categories, (An et al., 2022) introduced the FCDC task. Self-training approaches, such as Deep Cluster (Caron et al., 2018; An et al., 2023a), use clustering algorithms to detect the fine-grained categories, assign pseudo labels to the clusters and their samples, and then train

a classification model with these pseudo labels. Its variant, Deep Aligned Clustering (Zhang et al., 2021), devises a strategy to filter out inconsistent pseudo-labels during clustering. Contrastive learning has become prevalent in FCDC tasks; (Bukchin et al., 2021; An et al., 2022) developed angular contrastive learning tailored for fine-grained classification. An et al. (2022) proposed a weighted self-contrastive framework to enhance the model’s discriminative capacity for coarse-grained samples. (Ma et al., 2023) and (An et al., 2023a) used noisy fine-grained centroids and retrieved neighbors as positive pairs, respectively, applying constraints to filter noise. An et al. (2024) advanced this approach with neighbors that are manually weighted as positive pairs. However, previous efforts have not leveraged comprehensive semantic similarities to guide sample distributions and thereby to enhance fine-grained category discovery.

## 2.2 Neighborhood Contrastive Learning

Contrastive learning enhances representation learning by bringing the query sample closer to positive samples and distancing it from negative samples (Chen et al., 2020). Prior research has focused on constructing high-quality positive pairs. (He et al., 2020) utilized two different transformations of the same input as query and positive sample, respectively. Li et al. (2020) introduced the use of prototypes, derived through clustering, as positive instances. Additionally, An et al. (2022) employed shallow-layer features from BERT as positive samples and introduced a weighted contrastive loss. This approach primarily differentiates data at a coarse-grained level, and the manually set weights limit its broader applicability.

To circumvent complex data augmentation, neighborhood contrastive learning (NCL) was developed, treating the nearest neighbors of queries as positive samples (Dwibedi et al., 2021). Zhong et al. (2021) extended this by utilizing k-nearest neighbors to identify hard negative samples, while Zhang et al. (2022) selected a positive key from the k-nearest neighbors for contrastive representation learning. However, these approaches often deal with noisy nearest neighbors that include false-positive samples. (An et al., 2023a) addressed this by proposing three constraints to filter out uncertain neighbors, yet they overlooked semantic similarities between query sample and each available sample. An et al. (2024) represented semantic similarities using rank order among positive samples

but neglected similarities among negative samples. In contrast, STAR uses comprehensive semantic similarities to guide sample distributions in the Euclidean space, offering richer features and a superior approach to pure contrastive learning.

## 3 Problem Formulation

Given a set of coarse-grained categories  $Y_{coarse} = \{C_1, C_2, \dots, C_M\}$  and a coarsely labeled training set  $D_{train} = \{(x_i, c_i) \mid c_i \in Y_{coarse}\}_{i=1}^N$ , where  $N$  denotes the number of training samples, the task of FCDC involves developing a feature encoder  $F_\theta$ . This encoder maps samples into a feature space, further segmenting them into distinct fine-grained categories  $Y_{fine} = \{F_1, F_2, \dots, F_K\}$ , without any fine-grained supervisory information. Here,  $Y_{fine}$  represents sub-classes of  $Y_{coarse}$ . Model effectiveness is evaluated on a testing set  $D_{test} = \{(x_i, y_i) \mid y_i \in Y_{fine}\}_{i=1}^L$ , with  $L$  as the number of test samples, utilizing features extracted by  $F_\theta$ . For evaluation consistency and fairness, only the number of fine-grained categories  $K$  is used, aligning with methodologies established in previous research (Ma et al., 2023; An et al., 2022, 2023a).

## 4 Method

STAR leverages comprehensive semantic similarities and integrates seamlessly with contrastive learning baselines by modifying the objective function. We have developed variants for three baselines: PseudoPrototypicalNet (PPNet) (Boney and Ilin, 2017; Ji et al., 2020), DNA (An et al., 2023a), and DOWN (An et al., 2024). This section focuses on STAR-DOWN because DOWN outperforms other baselines, with additional method variants detailed in Appendix

DOWN involves three steps: pre-training with coarse-grained labels (Section 4.1), retrieving and weighting nearest neighbors (Section 4.2), and training with a contrastive loss. STAR-DOWN follows the same first two steps but replaces the third with a novel objective function (Section 4.3). Like DOWN, STAR-DOWN iterates the last two steps until the unsupervised metric, the silhouette score of the clustering into fine-grained clusters, does not improve for five consecutive epochs. The detailed algorithm is provided in Appendix

### 4.1 Multi-task Pre-training

As illustrated in Figure 3, the baseline DOWN (An et al., 2024) utilizes the BERT Encoder  $F_\theta$  to ex-

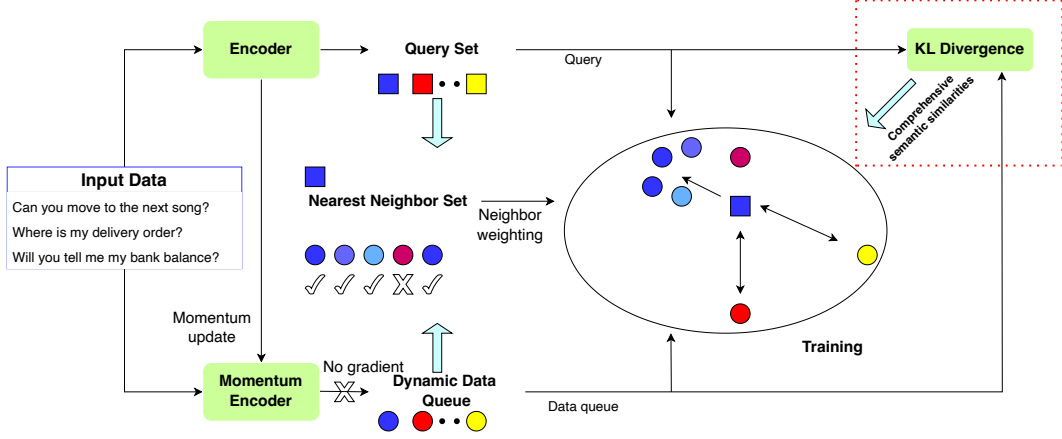


Figure 3: STAR-DOWN integrates the baseline DOWN with the STAR method (shown in the red dashed box). In the visual representation, colors differentiate samples, squares represent features extracted by the Encoder, and circles denote features extracted by the Momentum Encoder. Unidirectional arrows indicate proximity, while bidirectional arrows signify distance between samples.

tract normalized feature embeddings  $q_i = F_\theta(x_i)$  for input  $x_i$ , where  $\theta$  represents the Encoder parameters. To ensure effective initialization for fine-grained training, DOWN pre-trains the Encoder on the coarsely labeled train set  $D_{train}$  with labels  $Y_{coarse}$ . DOWN utilizes the sum of a cross-entropy loss  $L_{ce}$  and a masked language modeling loss  $L_{mlm}$  for multi-task pre-training of the Encoder (detailed in Appendix

## 4.2 Neighbors Retrieval and Weighting

In Figure 3, the Momentum Encoder  $F_{\theta_k}$  with parameters  $\theta_k$  extracts and stores gradient-free normalized neighbor features  $h_i = F_{\theta_k}(x_i)$  in a dynamic data queue  $Q$ . To ensure consistency between the outputs of  $F_{\theta_k}$  and  $F_\theta$ ,  $F_{\theta_k}$ 's parameters are updated via a moving-average method (He et al., 2020):  $\theta_k \leftarrow m\theta_k + (1 - m)\theta$ , where  $m$  is the momentum coefficient. For each query feature  $q_i$ , in order to facilitate semantic similarity capture and fine-grained clustering, its top- $k$  nearest neighbors  $N_i$  are determined from  $Q$  using cosine similarity (Sim):  $N_i = \{h_j \mid h_j \in \text{argtopK}_{h_l \in Q}(\text{Sim}(q_i, h_l))\}$ , where  $\text{Sim}(q_i, h_l) = \frac{q_i^T h_l}{\|q_i\| \cdot \|h_l\|}$  is the cosine similarity function.

To counteract potential false positives in  $N_i$ , DOWN utilizes a soft weighting mechanism based on neighbor rank to balance information utility against noise, with weights  $\omega_j$  of neighbor  $h_j$  calculated as:  $\omega_j = \phi \cdot \alpha^{-\frac{l_{ij}}{k}}$ , where  $\phi$  is a normalizing constant for weights,  $\alpha$  serves as the exponential base,  $k$  is the retrieved neighbor count, and  $l_{ij}$  denotes the rank of  $h_j$  as a neighbor to  $q_i$ .

To align with the model's evolving accuracy in neighbor retrieval during training, DOWN periodically decreases  $\alpha$  every five epochs, the values for  $\alpha$  in  $\omega_j$  are:  $\alpha_{set} = \{150, 10, 5, 2\}$ . The  $\omega_j$  of each positive sample  $h_j$  is used in Eqs. 3 and 4.

## 4.3 Training

### 4.3.1 Objective Function

Given a training batch  $N_{train} \in D_{train}$ , where  $Y_c$  is the set of coarse-grained labels of  $N_{train}$ , DOWN trains the model using the loss:

$$L_{train} = L_{ce} + L_{DOWN}, \quad (1)$$

$$L_{DOWN} = \frac{1}{|N_{train}|} \sum_{q_i \in N_{train}} L_1^i. \quad (2)$$

As shown in Eq. 3, DOWN uses a conventional contrastive objective function in the Euclidean space, while STAR-DOWN introduces a novel objective function in Eq. 4, leveraging CSS in a logarithmic space to guide sample distributions in the Euclidean space, the temperature  $\tau$  is a fixed constant in Eq. 3 and Eq. 4:

$$L_1^i = - \sum_{h_j \in N_i} \omega_j \cdot \log \frac{\exp(q_i^T h_j / \tau)}{\sum_{h_k \in Q} \exp(q_i^T h_k / \tau)}. \quad (3)$$

$$L_2^i = - \gamma \sum_{h_j \in N_i} \omega_j \cdot \log \frac{\exp(-d_{KL}(q_i, h_j) / \tau)}{\sum_{h_k \in Q} \exp(-d_{KL}(q_i, h_k) / \tau)} - \sum_{h_j \in N_i} \omega_j \cdot \log \frac{\exp(q_i^T h_j / \tau)}{\sum_{h_k \in Q} B^{d_{KL}(q_i, h_k)} \cdot \exp(q_i^T h_k / \tau)}. \quad (4)$$

During training, STAR-DOWN optimizes the following objective function:

$$L_{\text{train}} = L_{\text{ce}} + L_{\text{STAR}}, \quad (5)$$

$$L_{\text{STAR}} = \frac{1}{|N_{\text{train}}|} \sum_{q_i \in N_{\text{train}}} L_2^i. \quad (6)$$

As shown in Eq. 4, the term  $d_{KL}(q_i, h_k)$  in  $L_2^i$  represents the bidirectional KL divergence in a logarithmic space between the query sample embedding  $q_i$  and the data queue sample embedding  $h_k$  (detailed in Appendix B is a trainable scalar representing the exponential base.

The first term in  $L_2^i$  minimizes the KL divergence between query samples and positive samples (retrieved neighbors in Section 4.2) while increasing it for negative samples in the logarithmic space, with  $\gamma$  as a balancing hyperparameter. The second term in  $L_2^i$  uses CSS in the logarithmic space, denoted by  $B^{d_{KL}(q_i, h_k)}$ , to guide query sample distribution in the Euclidean space.  $q_i^T h_k$  quantifies the cosine similarity between normalized  $q_i$  and  $h_k$ , equivalent to the negative Euclidean distance (detailed in Appendix . The value of the trainable scalar  $B$  is updated during loss backpropagation, so  $B^{d_{KL}(q_i, h_k)}$  is fully trainable and can integrate with contrastive learning methods, making the STAR method *generic*.

### 4.3.2 Loss Analysis

Since STAR-DOWN discovers fine-grained categories in the Euclidean space, we analyze the second term  $L_{2-2}^i$  of the loss  $L_2^i$ , which optimizes sample distributions in the Euclidean space:

$$\begin{aligned} L_{2-2}^i &= - \sum_{h_j \in N_i} \omega_j \cdot \log \frac{\exp(q_i^T h_j / \tau)}{\sum_{h_k \in Q} B^{d_{KL}(q_i, h_k)} \cdot \exp(q_i^T h_k / \tau)} \\ &= \sum_{h_j \in N_i} \omega_j \cdot (\log \sum_{h_k \in Q} B^{d_{KL}(q_i, h_k)} \cdot \exp(q_i^T h_k / \tau) \\ &\quad - (q_i^T h_j / \tau)). \end{aligned} \quad (7)$$

In the loss  $L_{2-2}^i$ ,  $B^{d_{KL}(q_i, h_k)}$  uses CSS in the logarithmic space to guide sample distributions in the Euclidean space. A large  $d_{KL}(q_i, h_k)$  (low semantic similarity) causes  $q_i$  to distance itself from  $h_k$  in the Euclidean space, reducing  $q_i^T h_k$ , while a small  $d_{KL}(q_i, h_k)$  allows  $q_i$  to remain relatively close to  $h_k$  compared to negative samples. This results in the formation of compact fine-grained clusters, with each cluster representing a discovered category. We also analyze the STAR method

Dataset	$ \mathcal{C} $	$ \mathcal{F} $	# Train	# Test
CLINC	10	150	18000	1000
WOS	7	33	8362	2420
HWU64	18	64	8954	1031

Table 1: Statistics of datasets (An et al., 2023a). #: number of samples.  $|\mathcal{C}|$ : number of coarse-grained categories.  $|\mathcal{F}|$ : number of fine-grained categories.

from the perspectives of **gradient**, **clustering**, and **generalized EM**. Detailed analyses are provided in Appendix

## 4.4 Inference

Previous methods (An et al., 2023a, 2024) use clustering inference on sample embeddings from  $F_\theta$  extracted from  $D_{\text{test}}$ , which is unsuitable for real-time tasks, such as intent detection, which require immediate response and can not wait to collect enough test samples for clustering. We introduce an alternative, centroid inference, suitable for both real-time and other contexts. Using  $F_\theta$ , we derive sample embeddings from  $D_{\text{train}}$  and assign fine-grained pseudo labels through clustering. For each fine-grained cluster, only the embeddings of samples from the predominant coarse-grained category (the category with the most samples in this fine-grained cluster) are averaged to form centroid representations. These approximated centroids are used to determine the fine-grained category of each test sample based on cosine similarity. A visual explanation is in Appendix

## 5 Experiments

### 5.1 Experimental Settings

#### 5.1.1 Datasets

We conduct experiments on three benchmark datasets: CLINC (Larson et al., 2019), WOS (Kowsari et al., 2017), and HWU64 (Liu et al., 2021). CLINC is an intent detection dataset spanning multiple domains. WOS is used for paper abstract classification, and HWU64 is designed for assistant query classification. Dataset statistics are provided in Table 1.

#### 5.1.2 Baselines for Comparison

We compare our methods against the following baselines. **Language models:** BERT (Devlin et al., 2019b), BERT with coarse-grained fine-tuning, Llama2 (Touvron et al., 2023), Llama2 with coarse-grained fine-tuning and GPT4 (Achiam

et al., 2023). **Self-training** baselines: DeepCluster (DC) (Caron et al., 2018), DeepAlignedCluster (DAC) (Zhang et al., 2021), and PseudoPrototypicalNet (PPNet) (Boney and Ilin, 2017; Ji et al., 2020). **Contrastive learning** baselines: SimCSE (Gao et al., 2021), Ancor (Bukchin et al., 2021), Delete (Wu et al., 2020), Nearest-Neighbor Contrastive Learning (NNCL) (Dwibedi et al., 2021), Contrastive Learning with Nearest Neighbors (CLNN) (Zhang et al., 2022), Soft Neighbor Contrastive Learning (SNCL) (Chongjian et al., 2022), Weighted Self-Contrastive Learning (WSCL) (An et al., 2022), Denoised Neighborhood Aggregation (DNA), and Dynamic Order Weighted Network (DOWN) (An et al., 2023a, 2024). We also explore variants incorporating the cross-entropy loss (+CE).

### 5.1.3 Evaluation Metrics

To evaluate the quality of the discovered fine-grained clusters, we use the Adjusted Rand Index (ARI) (Hubert and Arabie, 1985) and Normalized Mutual Information (NMI) (Lancichinetti et al., 2009). For assessing classification performance, we use clustering Accuracy (ACC) (Kuh, 1955; An et al., 2023a). Detailed descriptions of these metrics are provided in Appendix

### 5.1.4 Implementation Details

To ensure fair comparisons with baselines, we use the BERT-base-uncased model as the backbone for all STAR method variants. We adhere to the hyperparameters used by the integrated baselines to demonstrate the effectiveness of our STAR method. The learning rate for both pre-training and training is  $5e^{-5}$ , using the AdamW optimizer with a 0.01 weight decay and 1.0 gradient clipping. The momentum coefficient  $m$  is set to 0.99. The batch size for pre-training, training, and testing is 64. The temperature  $\tau$  is set to 0.07. The number of neighbors  $k$  is set to  $\{120, 120, 250\}$  for the CLINC, HWU64, and WOS datasets, respectively. Epochs for pretraining and training are set to 100 and 20, respectively. Further details are provided in Appendix

### 5.1.5 Research Questions

The following research questions (RQs) are investigated: 1. What is the impact of STAR method on FCDC tasks? 2. What are the effects of the proposed real-time centroid inference compared to traditional clustering inference? 3. How does

each component of the STAR method affect performance? 4. How can we effectively and efficiently set the base for the exponential function in the STAR method?

## 5.2 Result Analysis (RQ1)

As shown in Table 2, STAR method variants outperform SOTA methods across all datasets and metrics, validating the effectiveness of the STAR method in FCDC tasks. Language models like BERT, Llama2 and GPT4 (Devlin et al., 2019b; Touvron et al., 2023; Achiam et al., 2023) (GPT4 prompt in Appendix ) perform poorly on the FCDC task due to the lack of fine-grained supervisory information. Self-training methods like DC, DAC, and PPNet (Caron et al., 2018; Zhang et al., 2021; Ji et al., 2020) also struggle because they rely on noisy fine-grained pseudo-labels and overlook comprehensive semantic similarities (CSS). Contrastive learning methods such as SNCL (Chongjian et al., 2022) and WSCL (An et al., 2022) perform better by leveraging positive pairs. DNA (An et al., 2023a) and DOWN (An et al., 2024) further enhance feature quality by filtering false positives and weighting them by rank. However, these methods still do not use CSS for sample distributions. Integrating the STAR method with existing baselines enhances performance across all datasets, consistently improving sample distributions in Euclidean space.

The superior performance of STAR is attributed to three factors: First, bidirectional KL divergence measures CSS, pushing negative samples further away and relatively bringing positive samples closer based on CSS magnitude, making fine-grained clusters easier to distinguish. Second, the base  $B$  of the exponential in Eq. 4 is a trainable scalar, balancing CSS magnitude and semantic structure. Third, STAR variants iteratively bootstrap model performance in neighborhood retrieval and representation learning through a generalized EM process (detailed in Appendix ).

## 5.3 Inference Mechanism Comparison (RQ2)

Previous methods (Chongjian et al., 2022; An et al., 2023a, 2024) perform a nearest neighbor search over the examples of the found fine-grained clusters for fine-grained category prediction (we refer to this technique as cluster inference). We speed up this process making it better suitable for real-time tasks by developing a centroid inference mechanism (see Section 4.4). Results in Table 3 demonstrates that results of centroid inference are compet-

Methods	HWU64			CLINC			WOS		
	ACC	ARI	NMI	ACC	ARI	NMI	ACC	ARI	NMI
BERT (Devlin et al., 2019b)	33.52	17.04	56.90	34.37	17.61	64.75	31.97	18.36	45.15
BERT + CE	37.89	33.68	74.63	43.85	32.37	78.58	38.29	36.94	64.72
Llama2 (Touvron et al., 2023)	19.27±1.21	5.21±0.46	44.34±0.85	20.77±2.61	5.83±1.52	49.7±3.68	9.85±1.14	1.26±0.75	18.27±2.28
Llama2 + CE	32.40±5.46	17.32±5.95	57.53±5.78	45.69±6.85	29.38±6.55	72.66±7.13	18.51±1.50	7.8±1.18	29.66±3.23
GPT4 (Achiam et al., 2023)	10.77±1.86	0.14±0.05	35.17±3.68	9.56±2.12	0.11±0.06	46.69±3.24	7.56±1.51	0.15±0.04	27.78±2.98
DC (Caron et al., 2018)	18.05	43.34	29.74	26.40	12.51	61.26	29.17	13.98	53.27
DAC (Zhang et al., 2021)	29.14	12.89	52.99	29.16	14.15	62.78	28.47	15.94	43.52
DC + CE	41.73	27.81	66.81	30.28	13.56	62.38	38.76	35.21	60.30
DAC + CE	42.19	28.15	66.50	42.09	28.09	72.78	39.42	33.67	61.60
PPNet (Ji et al., 2020)	58.36±2.51	47.63±1.96	79.75±1.02	70.15±1.86	59.31±0.96	85.08±0.81	62.59±1.41	50.81±1.21	72.19±0.68
<b>STAR-PPNet (ours)</b>	<b>63.19±2.38</b>	<b>52.21±1.33</b>	<b>81.66±1.21</b>	<b>73.21±1.97</b>	<b>61.87±0.79</b>	<b>86.16±0.47</b>	<b>66.15±1.33</b>	<b>53.61±1.24</b>	<b>73.82±0.74</b>
Delete (Wu et al., 2020)	21.30	6.52	44.13	47.11	31.28	73.39	24.50	11.68	35.47
SimCSE (Gao et al., 2021)	24.48	8.42	46.94	40.22	23.57	69.02	25.87	13.03	38.53
Ancor + CE	32.90	30.71	74.73	44.44	31.50	74.67	39.34	26.14	54.35
NNCL (Dwivedi et al., 2021)	32.98	30.02	73.24	17.42	13.93	67.56	29.64	28.51	61.37
SimCSE + CE	34.04	31.81	74.86	52.53	37.03	77.39	41.28	34.47	61.62
Delete + CE	35.13	31.84	74.88	47.87	33.79	76.25	41.53	33.78	61.01
CLNN (Zhang et al., 2022)	37.21	34.66	75.27	19.96	14.76	68.30	29.48	28.42	60.99
Ancor (Bukchin et al., 2021)	37.34	34.75	74.99	45.60	33.11	75.23	41.20	37.00	65.42
SNCL (Chongjian et al., 2022)	42.32	38.17	76.39	55.01	45.64	82.93	36.27	33.62	62.35
WSCL (An et al., 2022)	59.52	49.34	79.31	74.02	62.98	88.37	65.27	51.78	72.46
DNA (An et al., 2023a)	70.81	59.66	83.31	87.66	81.82	94.69	74.57	63.30	76.86
<b>STAR-DNA (ours)</b>	<b>75.79±0.93</b>	<b>65.27±1.12</b>	<b>85.34±0.36</b>	<b>89.25±0.17</b>	<b>83.47±0.27</b>	<b>95.11±0.05</b>	<b>77.19±0.81</b>	<b>64.97±0.75</b>	<b>77.91±0.76</b>
DOWN (An et al., 2024)	78.92	68.17	86.22	91.79	86.70	96.05	80.00	67.09	78.87
<b>STAR-DOWN (ours)</b>	<b>80.31±0.26</b>	<b>70.22±0.59</b>	<b>87.28±0.31</b>	<b>92.45±0.38</b>	<b>87.05±0.17</b>	<b>96.20±0.07</b>	<b>81.98±0.67</b>	<b>69.27±0.60</b>	<b>79.99±0.40</b>

Table 2: The average performance (%) in terms of Accuracy (ACC), Adjusted Rand Index (ARI), and Normalized Mutual Information (NMI) on three datasets for the FCDC language task. To ensure fair comparisons with previous works (An et al., 2022, 2023a, 2024) and demonstrate the effectiveness of STAR, we use the same clustering inference mechanism and also average the results over three runs with identical common hyperparameters. Some baselines results are cited from aforementioned previous works, where standard deviations are not originally provided.

Methods	HWU64			CLINC			WOS		
	ACC	ARI	NMI	ACC	ARI	NMI	ACC	ARI	NMI
STAR-DOWN (clustering)	80.31±0.26	70.22±0.59	87.28±0.31	92.45±0.38	87.05±0.17	96.20±0.07	81.98±0.67	69.27±0.60	79.99±0.40
STAR-DOWN (centroid)	79.44±0.51	69.13±0.75	86.97±0.40	92.60±0.45	87.16±0.53	96.21±0.09	81.89±0.53	69.05±0.39	79.78±0.32

Table 3: Comparison of clustering and centroid inference mechanisms. "Clustering" clusters test set sample embeddings to determine each sample’s fine-grained category, while "Centroid" infers the category by comparing each test sample’s cosine similarity to fine-grained centroids.

Methods	ACC	ARI	NMI
<b>ours</b>	80.31±0.26	70.22±0.59	87.28±0.31
w/o CE	78.61±0.44	67.32±0.86	85.62±0.36
w/o KL loss	78.97±0.32	68.03±0.36	85.81±0.16
w/o KL weight	79.26±0.42	68.86±0.37	86.21±0.07
w/o KL weight and loss	78.96±0.15	68.21±0.22	86.32±0.10

Table 4: Results (%) of the ablation study for STAR-DOWN on the HWU64 Dataset.

itive with cluster inference. When results are of the former are lower, this is due to two factors: clustering inference leverages inter-relations among test set samples for richer features, while centroid inference depends on centroids derived from noisy samples with fine-grained pseudo-labels. Despite these issues, centroid inference remains a viable option for real-time applications, balancing immediate analytical needs with slight performance trade-offs.

## 5.4 Ablation Study (RQ1 & RQ3)

We examine the impact of various components of the STAR method in STAR-DOWN, as detailed in Table 4. Our results yield the following insights. (1) Excluding coarse-grained supervision information during training (w/o CE) reduces model performance, as this information is crucial for effective representation learning. (2) Omitting the first loss term (w/o KL loss) from Eq. 4 diminishes performance. The KL loss term aligns the KL divergence between data samples and the query with their semantic similarities. Without it,  $B^{d_{KL}(q_i, h_k)}$  fails to guide the query sample distribution based on semantic similarities in Eq. 4. (3) Removing the KL weight  $B^{d_{KL}(q_i, h_k)}$  from Eq. 4 (w/o KL weight) reduces effectiveness. The loss no longer utilizes fine-grained semantic similarities measured by  $B^{d_{KL}(q_i, h_k)}$  in the logarithmic space to direct the query sample distribution in comparison to all

Base value	ACC	ARI	NMI
trainable $B$ (ours)	80.31±0.26	70.22±0.59	87.28±0.31
$e$	79.96±0.12	68.89±0.55	86.66±0.10
10	80.22±0.27	69.61±0.65	87.08±0.30
16	80.73±0.32	70.14±0.58	87.25±0.36
66	80.57±0.38	70.20±0.52	87.07±0.15

Table 5: Averaged results (%) and their standard deviations over three runs of multiple STAR-DOWN methods with **five different base values** on the HWU64 dataset. To set base value conveniently, we set  $B$  as a trainable scalar.

samples. (4) Eliminating both the KL loss term and the KL weight in Eq. 4 leads to a performance decline. This omission prevents the optimization of the query sample towards positive samples in the logarithmic space and fails to leverage fine-grained semantic similarities in logarithmic space to influence the distribution of query samples relative to all samples in the Euclidean space.

### 5.5 Exponential Base Impact (RQ4)

In the STAR method’s loss equation (Eq. 4),  $B^{d_{KL}(q_i, h_k)}$  modulates the distribution of  $q_i$  and  $h_k$  in the Euclidean space based on their semantic similarity in the logarithmic space, as quantified by the bidirectional KL divergence. The base  $B$  is used to enhance semantic differences, improving the discriminability of fine-grained categories. We experimented with multiple constant values and a trainable configuration for  $B$ , with multiple STAR-DOWN results presented in Table 5. The multiple STAR-DOWN methods with various base values consistently outperform the DOW method (Table 2), demonstrating the effectiveness and robustness of the STAR method regardless of the base value  $B$ .<sup>1</sup> Notably, base values that are either too low (e.g.,  $e$ ) or too high (e.g., 66) disrupt the semantic representation by inadequately or excessively emphasizing semantic similarities in the logarithmic space. To set base value conveniently, we set  $B$  as a trainable scalar, achieving favorable outcomes as indicated in Table 5.

### 5.6 Inference of Category Semantics

Prior works (An et al., 2023a, 2024) only discovered fine-grained categories and assigned them numeric indices without elucidating the categories semantics, thus constraining their broader application. We propose utilizing the commonsense reasoning

<sup>1</sup>For interesting form similarities to physical laws within the STAR method, see Appendix .

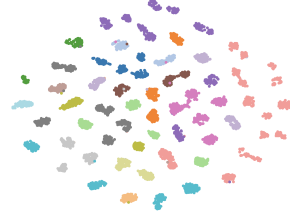


Figure 4: The t-SNE visualization of sample embeddings from STAR-DOWN method on the HWU64 dataset, with different colors representing different coarse-grained categories. The distinct clusters represent the discovered fine-grained categories.

capabilities of large language models (LLMs) to infer the semantics of these categories. Specifically, we employ a trained encoder,  $F_\theta$ , to extract embeddings from all train set samples and cluster these embeddings to assign fine-grained pseudo-labels to each train set sample. For each fine-grained category indicated by a specific pseudo-label, we aggregate all predicted samples from the training set and use an LLM to deduce the category semantics. Details on the LLM prompt are provided in Appendix .

### 5.7 Visualization

We visualize the sample embeddings of STAR-DOWN in Figure 4. The results demonstrate that our method forms distinguishable clusters for fine-grained categories, proving STAR’s effectiveness in separating dissimilar samples and clustering similar ones. Additionally, we visualize the generalized EM perspective of STAR-DOWN in Appendix .

## 6 Conclusion

We propose the STAR method for fine-grained category discovery in natural language texts, which utilizes comprehensive semantic similarities in the logarithmic space to guide the distribution of textual samples, including conversational intents, scientific paper abstracts, and assistant queries, in the Euclidean space. STAR pushes query samples further away from negative samples and brings them closer to positive samples based on the comprehensive semantic similarities magnitude. This process forms compact clusters, each representing a discovered category. We theoretically analyze the effectiveness of STAR method. Additionally, we introduce a centroid inference mechanism that addresses previous gaps in real-time evaluations. Experiments on three natural language benchmarks



demonstrate that STAR achieves new state-of-the-art performance in fine-grained category discovery tasks for text classification.

## References

1955. The hungarian method for the assignment problem. *Naval research logistics quarterly*, 2(1-2):83–97.
- Josh Achiam, Steven Adler, Sandhini Agarwal, Lama Ahmad, Ilge Akkaya, Florencia Leoni Aleman, Diogo Almeida, Janko Altenschmidt, Sam Altman, Shyamal Anadkat, et al. 2023. Gpt-4 technical report. *arXiv preprint arXiv:2303.08774*.
- Wenbin An, Feng Tian, Ping Chen, Siliang Tang, Qinghua Zheng, and Qianying Wang. 2022. Fine-grained category discovery under coarse-grained supervision with hierarchical weighted self-contrastive learning. In *Proceedings of the 2022 Conference on Empirical Methods in Natural Language Processing*, pages 1314–1323.
- Wenbin An, Feng Tian, Wenkai Shi, Yan Chen, Qinghua Zheng, Qianying Wang, and Ping Chen. 2023a. Dna: Denoised neighborhood aggregation for fine-grained category discovery. In *Proceedings of the 2023 Conference on Empirical Methods in Natural Language Processing*, pages 12292–12302.
- Wenbin An, Feng Tian, Wenkai Shi, Haonan Lin, Yaqiang Wu, Mingxiang Cai, Luyan Wang, Hua Wen, Lei Yao, and Ping Chen. 2024. Down: Dynamic order weighted network for fine-grained category discovery. *Knowledge-Based Systems*, 293:111666.
- Wenbin An, Feng Tian, Qinghua Zheng, Wei Ding, Qianying Wang, and Ping Chen. 2023b. Generalized category discovery with decoupled prototypical network. In *Proceedings of the AAAI Conference on Artificial Intelligence*, volume 37, pages 12527–12535.
- Rinu Boney and Alexander Ilin. 2017. Semi-supervised and active few-shot learning with prototypical networks. *arXiv preprint arXiv:1711.10856*.
- Guy Bukchin, Eli Schwartz, Kate Saenko, Ori Shahar, Rogerio Feris, Raja Giryes, and Leonid Karlinsky. 2021. Fine-grained angular contrastive learning with coarse labels. In *Proceedings of the IEEE/CVF conference on computer vision and pattern recognition*, pages 8730–8740.
- Mathilde Caron, Piotr Bojanowski, Armand Joulin, and Matthijs Douze. 2018. Deep clustering for unsupervised learning of visual features. In *Proceedings of the European conference on computer vision (ECCV)*, pages 132–149.
- Tianshui Chen, Liang Lin, Riquan Chen, Yang Wu, and Xiaonan Luo. 2018. Knowledge-embedded representation learning for fine-grained image recognition. In *Proceedings of the 27th International Joint Conference on Artificial Intelligence*, pages 627–634.
- Ting Chen, Simon Kornblith, Mohammad Norouzi, and Geoffrey Hinton. 2020. A simple framework for contrastive learning of visual representations. In *International conference on machine learning*, pages 1597–1607. PMLR.
- GE Chongjian, Jiangliu Wang, Zhan Tong, Shoufa Chen, Yibing Song, and Ping Luo. 2022. Soft neighbors are positive supporters in contrastive visual representation learning. In *The Eleventh International Conference on Learning Representations*.
- Jacob Devlin, Ming-Wei Chang, Kenton Lee, and Kristina Toutanova. 2019a. Bert: Pre-training of deep bidirectional transformers for language understanding. In *Proceedings of the 2019 Conference of the North American Chapter of the Association for Computational Linguistics: Human Language Technologies, Volume 1 (Long and Short Papers)*, pages 4171–4186.
- Jacob Devlin, Ming-Wei Chang, Kenton Lee, and Kristina Toutanova. 2019b. [BERT: Pre-training of deep bidirectional transformers for language understanding](#). In *Proceedings of the 2019 Conference of the North American Chapter of the Association for Computational Linguistics: Human Language Technologies, Volume 1 (Long and Short Papers)*, pages 4171–4186, Minneapolis, Minnesota. Association for Computational Linguistics.
- Debidatta Dwivedi, Yusuf Aytar, Jonathan Tompson, Pierre Sermanet, and Andrew Zisserman. 2021. With a little help from my friends: Nearest-neighbor contrastive learning of visual representations. In *Proceedings of the IEEE/CVF International Conference on Computer Vision*, pages 9588–9597.
- Tianyu Gao, Xingcheng Yao, and Danqi Chen. 2021. Simcse: Simple contrastive learning of sentence embeddings. In *Proceedings of the 2021 Conference on Empirical Methods in Natural Language Processing*, pages 6894–6910.
- Xiaoting Guo, Wei Yu, and Xiaodong Wang. 2021. An overview on fine-grained text sentiment analysis: Survey and challenges. In *Journal of Physics: Conference Series*, volume 1757, page 012038. IOP Publishing.
- Kaiming He, Haoqi Fan, Yuxin Wu, Saining Xie, and Ross Girshick. 2020. Momentum contrast for unsupervised visual representation learning. In *Proceedings of the IEEE/CVF conference on computer vision and pattern recognition*, pages 9729–9738.
- Lawrence Hubert and Phipps Arabie. 1985. Comparing partitions. *Journal of classification*, 2:193–218.
- Zilong Ji, Xiaolong Zou, Tiejun Huang, and Si Wu. 2020. Unsupervised few-shot feature learning via self-supervised training. *Frontiers in computational neuroscience*, 14:83.

- Kamran Kowsari, Donald E Brown, Mojtaba Heidarysafa, Kiana Jafari Meimandi, Matthew S Gerber, and Laura E Barnes. 2017. Hdltext: Hierarchical deep learning for text classification. In *2017 16th IEEE international conference on machine learning and applications (ICMLA)*, pages 364–371. IEEE.
- Andrea Lancichinetti, Santo Fortunato, and János Kertész. 2009. Detecting the overlapping and hierarchical community structure in complex networks. *New journal of physics*, 11(3):033015.
- Stefan Larson, Anish Mahendran, Joseph J Peper, Christopher Clarke, Andrew Lee, Parker Hill, Jonathan K Kummerfeld, Kevin Leach, Michael A Laurenzano, Lingjia Tang, et al. 2019. An evaluation dataset for intent classification and out-of-scope prediction. In *Proceedings of the 2019 Conference on Empirical Methods in Natural Language Processing and the 9th International Joint Conference on Natural Language Processing (EMNLP-IJCNLP)*, pages 1311–1316.
- Junnan Li, Pan Zhou, Caiming Xiong, and Steven Hoi. 2020. Prototypical contrastive learning of unsupervised representations. In *International Conference on Learning Representations*.
- Ruixue Lian, William A Sethares, and Junjie Hu. 2024. Learning label hierarchy with supervised contrastive learning. *arXiv preprint arXiv:2402.00232*.
- Xingkun Liu, Arash Eshghi, Pawel Swietojanski, and Verena Rieser. 2021. Benchmarking natural language understanding services for building conversational agents. In *Increasing Naturalness and Flexibility in Spoken Dialogue Interaction: 10th International Workshop on Spoken Dialogue Systems*, pages 165–183. Springer.
- Ruotian Ma, Zhang Lin, Xuanting Chen, Xin Zhou, Junzhe Wang, Tao Gui, Qi Zhang, Xiang Gao, and Yun Wen Chen. 2023. Coarse-to-fine few-shot learning for named entity recognition. In *Findings of the Association for Computational Linguistics: ACL 2023*, pages 4115–4129.
- Dheeraj Mekala, Varun Gangal, and Jingbo Shang. 2021. Coarse2fine: Fine-grained text classification on coarsely-grained annotated data. In *Proceedings of the 2021 Conference on Empirical Methods in Natural Language Processing*, pages 583–594.
- Zhengxin Pan, Fangyu Wu, and Bailing Zhang. 2023. Fine-grained image-text matching by cross-modal hard aligning network. In *Proceedings of the IEEE/CVF conference on computer vision and pattern recognition*, pages 19275–19284.
- Wongi Park and Jongbin Ryu. 2024. Fine-grained self-supervised learning with jigsaw puzzles for medical image classification. *Computers in Biology and Medicine*, page 108460.
- Chang Tian, Wenpeng Yin, Dan Li, and Marie-Francine Moens. 2024. Fighting against the repetitive training and sample dependency problem in few-shot named entity recognition. *IEEE Access*.
- Hugo Touvron, Thibaut Lavril, Gautier Izacard, Xavier Martinet, Marie-Anne Lachaux, Timothée Lacroix, Baptiste Rozière, Naman Goyal, Eric Hambro, Faisal Azhar, et al. 2023. Llama: Open and efficient foundation language models. *arXiv preprint arXiv:2302.13971*.
- Sagar Vaze, Andrea Vedaldi, and Andrew Zisserman. 2024. No representation rules them all in category discovery. *Advances in Neural Information Processing Systems*, 36.
- Shijie Wang, Jianlong Chang, Zhihui Wang, Haojie Li, Wanli Ouyang, and Qi Tian. 2024a. Content-aware rectified activation for zero-shot fine-grained image retrieval. *IEEE Transactions on Pattern Analysis and Machine Intelligence*.
- Shijie Wang, Zhihui Wang, Haojie Li, Jianlong Chang, Wanli Ouyang, and Qi Tian. 2024b. Accurate fine-grained object recognition with structure-driven relation graph networks. *International Journal of Computer Vision*, 132(1):137–160.
- Zhuofeng Wu, Sinong Wang, Jiatao Gu, Madian Khabsa, Fei Sun, and Hao Ma. 2020. Clear: Contrastive learning for sentence representation. *arXiv preprint arXiv:2012.15466*.
- Hanlei Zhang, Hua Xu, Ting-En Lin, and Rui Lyu. 2021. Discovering new intents with deep aligned clustering. In *Proceedings of the AAAI Conference on Artificial Intelligence*, volume 35, pages 14365–14373.
- Yuwei Zhang, Haode Zhang, Li-Ming Zhan, Xiao-Ming Wu, and Albert Lam. 2022. New intent discovery with pre-training and contrastive learning. In *Proceedings of the 60th Annual Meeting of the Association for Computational Linguistics (Volume 1: Long Papers)*, pages 256–269.
- Zhun Zhong, Enrico Fini, Subhankar Roy, Zhiming Luo, Elisa Ricci, and Nicu Sebe. 2021. Neighborhood contrastive learning for novel class discovery. In *Proceedings of the IEEE/CVF conference on computer vision and pattern recognition*, pages 10867–10875.